

Monte Carlo Simulation of Cisplatin Molecule in Aqueous Solution

Juliana Fedoce Lopes,[†] Victor Ströele de A. Menezes,[†] Hélio A. Duarte,[‡] Willian R. Rocha,[§] Wagner B. De Almeida,[§] and Hélio F. Dos Santos*,[†]

NEQC: Núcleo de Estudos em Química Computacional, Departamento de Química, ICE, Universidade Federal de Juiz de Fora, Campus Martelos, CEP 36036-900, Juiz de Fora, MG, Brazil, GPQIT: Grupo de Pesquisa em Química Inorgânica Teórica, Departamento de Química, ICEx, Universidade Federal de Minas Gerais, Campus Pampulha, CEP 31270-901, Belo Horizonte, MG, Brazil, and LQC-MM: Laboratório de Química Computacional e Modelagem Molecular, Departamento de Química, ICEx, Universidade Federal de Minas Gerais, Campus Pampulha, CEP 31270-901, Belo Horizonte, MG, Brazil

Received: December 22, 2005; In Final Form: April 22, 2006

The Lennard-Jones (12–6) parameters were obtained for all atoms of cisplatin molecule using the ab initio quantum mechanical potential energy surface for the water–cisplatin interaction as reference data. The parameters found were ($\epsilon/\text{kcal}\cdot\text{mol}^{-1}$ and $\sigma/\text{\AA}$) 1.0550, 3.6590 (Pt); 0.0381, 4.6272 (Cl); 0.0455, 3.3783 (N); and 0.0185, 0.0936 (H) and provided very good results for the description of the aqueous solution of cisplatin through Monte Carlo simulation. From statistical analysis of solute–solvent interactions, we observed that the NH_3 groups are involved in 53% of the calculated hydrogen bonds with a significant contribution from chlorides (41%) and only 6% involving the Pt center. This is in agreement with the expected behavior for such molecules. Two hydration shells with 22 and 81 water molecules, respectively, centered around 4.6 and 7.3 \AA were found from the center of mass pair correlation function analysis. The cisplatin atomic Lennard-Jones parameters are reported for the first time, and they might be useful for studying the structure, properties, and processes of cisplatin-like molecules in aqueous solution, including explicitly the solvent effect.

Introduction

Compounds such as *cis*-diamminedichloroplatinum(II), cisplatin (*cis*-DDP), and their derivatives have been studied widely in several areas of chemistry and other sciences because of their biological value. It has been well known since 1965, after the pioneer work of Rosenberg,^{1,2} that these compounds act with effectiveness against neoplastic diseases such as all kinds of cancers. The antineoplastic properties of platinum-based complexes are strongly related to their spatial arrangement; square-planar geometry and *cis* configuration.^{3,4} Despite the intense research with the cisplatin derivatives, their action mechanism is still not completely understood. It is recognized that the final step is the interaction with the DNA molecule, through an associative process with the nitrogen atoms of the purine bases.^{5–7} The coordination of the platinum to DNA leads to physical and chemical modifications in the DNA structure, interfering in the cell functions. However, it is believed that some preliminary steps occur before reaching the final target, which are important to the efficacy of the drug, such as the interaction with sulfur-containing biomolecules^{8,9} and the aquation process.^{5,10} The latter has been considered to play a primary role in the action mechanism of these metalodrugs because only monoquo and diaquo species can interact with DNA effectively.¹¹ The thermodynamics and kinetics of the aquation process have been investigated using experimental techniques^{12–17} and theoretical approaches,^{18–22} aiming to characterize the mechanism and find correlations between chemical properties

and biological response. We have recently shown²¹ a good example of a quantitative relationship (QSAR) involving the aquation rate constant and electronic descriptors for a series of cisplatin derivatives. This QSAR analysis has been discussed regarding to the mutagenic power of these compounds (see also ref 23).

Most of the calculations of cisplatin derivatives have been carried out in the gas phase or in solution using polarizable continuum models (PCM).^{18–22} In a recent review,²⁴ Rotzinger suggests the need for inclusion of the solvent effect to properly reproduce the geometry and observed kinetic properties. Therefore, the quantitative description of the solute–solvent interactions is important in order to understand the effects of the medium for such processes at a molecular level. Besides the continuum models, which are restricted to the bulk solvent effect, molecular dynamics (MD) and Monte Carlo (MC) simulations can be used to account for specific solute–solvent interactions.^{25–28} A recent quantum mechanical DFT Car–Parrinello MD simulation of cisplatin in water was reported by Carloni and co-workers²⁹ considering 35 water molecules. Classical MD simulations have also been described by Naidoo and colleagues^{30,31} for the related platinum complexes $[\text{PtCl}_6]^{2-}$ and $[\text{PtCl}_4]^{2-}$. A recent paper on solvation of cisplatin was reported by Robertazzi and Platts²⁰ using the cluster approach at the DFT level to include explicitly the solvent effect. Dobrogorskaia-Méreau and Nemukhin³² used hybrid quantum mechanical/molecular mechanics (QM/MM) to study the reduction process of the Pt(IV) complex in aqueous solution with the environment modeled by 82 water molecules treated classically. In addition, Zhu and colleagues³³ reported recently a theoretical study of the aquation process of the JM118 third generation analogue using distinct approaches to model the

* Corresponding author. E-mail: helius@quimica.ufjf.br. Fax: +55 32 3229-3314.

[†] NEQC.

[‡] GPQIT.

[§] LQC-MM.

medium effects. They concluded that the explicit solvent molecules play an important role in the structure and energy of the species involved in the hydrolysis reaction and also suggest that a larger model must be used to a more accurate description of this process. The square-planar Pt(II) aquaion, $[\text{Pt}(\text{H}_2\text{O})_4]^{2+}$, has been studied in water solution by means of MD simulation³⁴ and a new concept of *meso-shell* was introduced to define the hydration pattern on the axial region. Important outcomes have been raised from these studies even though a complete description of the solution structure of cisplatin-like molecules has still to be achieved.

In the present work, the parameters for the Lennard-Jones (12–6) plus coulomb pair potential were derived for all atoms on the cisplatin molecule and used in the MC simulation to describe the aqueous solution process. This is the first time that ϵ and σ parameters are reported for all atoms on cisplatin, including the Pt center. The importance of these parameters for further studies of the chemical reaction and the molecular properties of other cisplatin-like molecules in water solution are discussed briefly.

Calculations

Parametrization Procedure. Geometry optimizations were performed at the second-order Møller–Plesset perturbation level of theory (MP2), within the frozen core approach (MP2(FC)), employing the split-valence 6-31G(d,p) basis set for the ligands^{35,36} and the relativistic effective core potential (ECP) and associated valence double- ζ basis set developed by Hay and Wadt (LANL2DZ) for Pt.³⁷ The parametrization protocol followed the general procedure as described by Norrby and Brandt.³⁸ The Lennard-Jones (12–6) plus Coulomb potential (1) was chosen to describe the interaction between cisplatin and water molecules in solution. This intermolecular potential is commonly used for liquid simulation and provides a reasonable description of the solute properties in solution.³⁹

$$U_{cl}^k(r_{ij}) = 4\epsilon_{ij} \left[\left(\frac{\sigma_{ij}}{r_{ij}} \right)^{12} - \left(\frac{\sigma_{ij}}{r_{ij}} \right)^6 \right] + \frac{q_i q_j}{r_{ij}} \quad (1)$$

The parameters σ_{ij} and ϵ_{ij} were calculated as a geometrical average, $\sigma_{ij} = (\sigma_i \sigma_j)^{1/2}$ and $\epsilon_{ij} = (\epsilon_i \epsilon_j)^{1/2}$, with the values of σ_i and ϵ_i obtained for all atoms of cisplatin, keeping the values for water atoms the same as those from the TIP3P model.⁴⁰ For the cisplatin molecule, the charges were calculated using the ChelpG fitting procedure.⁴¹ The reference data were the potential energy curves (PEC) calculated for distinct orientations of the cisplatin–water system (Figure 1), with each molecule fixed in its MP2/6-31G(d,p)/LANL2DZ optimized geometry. For each path shown in Figure 1, a collection of energy calculations was carried out for a set of 40 separation distances between the monomers without orientational changes. The quantum mechanical interaction energy (U_Q^k) was obtained for every configuration k from the difference between the total energy of the dimer and the sum of total energies of cisplatin and water, with and without correction for the basis-set superposition error (BSSE). The BSSE correction was included by using the counterpoise procedure.⁴²

The large amount of data was fitted to the Lennard-Jones (12–6) plus Coulomb potential (1) using the method of *quasi-Newton*⁴³ implemented in our laboratories. The penalty function (f) was defined as eq 2, where N is the total number of data

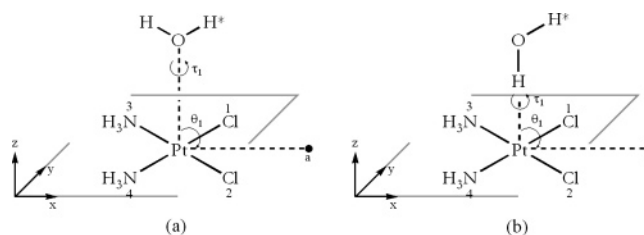


Figure 1. Distinct orientations of the cisplatin–water system used to calculate the potential energy curves. The cisplatin molecule is on the xy plane, and the water molecule is represented along the z axis. The orientational parameters were defined as τ_1 : $[\text{H}^*, \text{O}, \text{Pt}, a]$ and θ_1 : $[\text{O}, \text{Pt}, a]$, a being a dummy center along the x axis. (a) PEC1 (plane xz , $\tau_1 = 0.0^\circ$, $\theta_1 = 90.0^\circ$); PEC3 (plane xy , $\tau_1 = 180.0^\circ$, $\theta_1 = 0.0^\circ$); PEC4 (plane xy , $\tau_1 = 0.0^\circ$, $\theta_1 = 180.0^\circ$); PEC5 (plane xy , $\tau_1 = 90.0^\circ$, $\theta_1 = 90.0^\circ$). (b) PEC2 (plane xz , $\tau_1 = 0.0^\circ$, $\theta_1 = 90.0^\circ$); PEC6 (plane xy , $\tau_1 = 180.0^\circ$, $\theta_1 = 0.0^\circ$); PEC7 (plane xy , $\tau_1 = 0.0^\circ$, $\theta_1 = 180.0^\circ$); PEC8 (plane xy , $\tau_1 = 90.0^\circ$, $\theta_1 = 90.0^\circ$). Plane ij is parallel to the Pt–O bond vector.

TABLE 1: Intermolecular Lennard-Jones (12–6) Potential Parameters for Cisplatin (Present Work) and Water (TIP3P)

	$\epsilon/\text{kcal}\cdot\text{mol}^{-1}$	$\sigma/\text{\AA}$	q^b/au
Pt	1.0550	3.6590	0.06905
Cl	0.0381	4.6272	−0.37495
N	0.0455	3.3783	−0.41047
H1	0.0185	0.0936	0.23882
H2	0.0185	0.0936	0.25604
O ^a	0.152	3.151	−0.834
H ^a	0.000	0.000	0.417

^a TIP3P model.⁴⁰ ^b MP2/6-31G(d,p)/LANL2DZ ChelpG charges for cisplatin atoms.

and w^k is a weight factor, set constant and equal to 1 $\text{kcal}^{-2}\cdot\text{mol}^2$.

$$f(\sigma_{ij}, \epsilon_{ij}) = \frac{1}{N} \sum_{k=1}^N w^k [U_{cl}^k(\sigma_{ij}, \epsilon_{ij}) - U_Q^k]^2 \quad (2)$$

It is important to note that the Lennard-Jones parameters for all of the atoms of cisplatin were fitted simultaneously, and therefore they have to be used as a unique set.

The quantum mechanical calculations were carried out using the Gaussian 03 revision B.05 suite program⁴⁴ installed in the computers of the Núcleo de Estudos em Química Computacional (NEQC-DQ-UFJF).

Monte Carlo Simulation. The Monte Carlo (MC) simulation was carried out using standard procedures, including the Metropolis sampling technique and periodic boundary conditions with the minimum image method^{39,45} in a cubic box ($L = 31.2$ Å). The canonical NVT ensemble was considered with the system under investigation consisting of 1 cisplatin and 1000 water molecules. The volume of the cubic box was obtained from the experimental density of water, which is $0.997 \text{ g}\cdot\text{cm}^{-3}$ at $T = 298.15$ K. The intermolecular interactions were described by the Lennard-Jones plus Coulomb potential shown in eq 1 with three parameters for each atom (ϵ_i , σ_i , and q_i) (Table 1). For the cisplatin atoms the set of parameters was obtained in the present work, and for water the TIP3P model⁴⁰ was used. The intermolecular interactions were spherically truncated within a cutoff radius of 15.6 Å (half of the box length), and long-range corrections were calculated beyond this cutoff distance.^{39,46} During the simulation, the solute and solvent molecules were kept with rigid geometries, the cisplatin was held rigid in its MP2/6-31G(d,p)/LANL2DZ optimized structure, and the water molecule was held in a C_{2v} geometry with $r_{\text{OH}} = 0.9572$ Å and $\angle\text{HOH} = 104.52^\circ$.⁴⁰

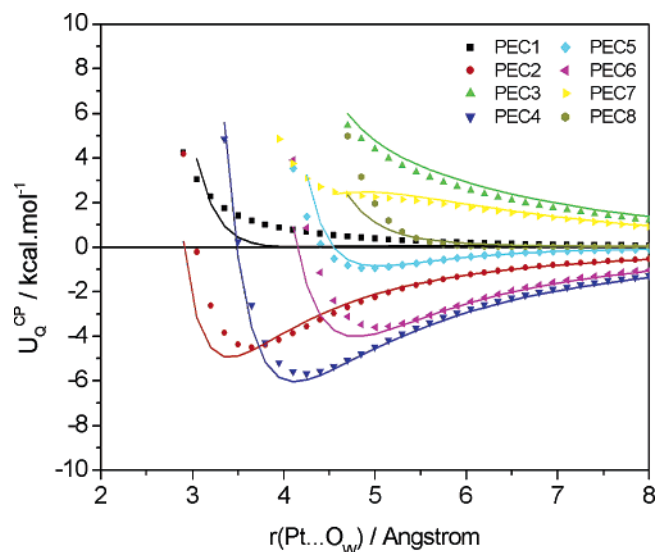


Figure 2. Potential energy curves calculated for the cisplatin–water system at the MP2/6-31G(d,p)/LANL2DZ level of theory including the BSSE correction. The solid line is the classical potential adjusted in the present work. The structural arrangements are defined in Figure 1.

The equilibration phase entailed 30 000 MC steps, and the averaging configuration phase entailed 150 000 MC steps, where 1 MC step is taken after all solvent molecules sequentially attempt to translate in all Cartesian directions and also attempt to rotate around a randomly chosen axis. The site–site radial distribution functions $[g(r)]$ were calculated every 5 MC steps, and the configurations for subsequent analysis were stored every 200 MC steps. The MC simulations were done with the DICE suite program developed and implemented by Coutinho and Canuto.⁴⁷

Results and Discussion

The MP2/6-31G(d,p)/LANL2DZ optimized geometry for cisplatin agreed fairly well with the experimental data. The Pt–Cl and Pt–N bonds were only 0.01 and 0.08 Å longer than those found in ref 48. For the bond angles, the deviations are within 10°. For the water molecules, the MP2/6-31G(d,p) optimized structure ($r_{OH} = 0.960$ Å and $\angle HOH = 103.98^\circ$) was also found to be in good accordance with the experiment ($r_{OH} = 0.958$ Å and $\angle HOH = 104.50^\circ$)⁴⁹ and TIP3P model ($r_{OH} = 0.9572$ Å and $\angle HOH = 104.52^\circ$).⁴⁰ The geometry dependence on the basis set was taken into account by optimizing the *cis*-DDP structure at the MP2/6-31++G(d,p)/LANL2DZ level and also including a set of seven *f* functions ($\alpha_f = 0.9804$) for the description of the Pt atom as suggested by Burda and co-workers.^{50–51} The deviations from our level of theory were lower than 0.03 Å and 0.4° for bond lengths and angles, respectively. The effect was also small for the cisplatin–water interaction energy as will be shown in the following paragraphs.

The calculated PECs for the distinct orientations depicted in Figure 1 are shown in Figure 2, with the quantum mechanical interaction energy corrected for BSSE (U_Q^{CP}) plotted against $r(\text{Pt}\cdots\text{O}_w)$ distance. In PECs 1 and 2, the water approaches to cisplatin through the *z* axis (Figure 1a and b), and for the other PECs analyzed the cisplatin–water interactions were in the cisplatin plane (*xy*) (see Figure 1). Table 2 gives the equilibrium distance and interaction energy for all curves with and without including the BSSE correction. The BSSE is quite significant, amounting to at least 40% of the interaction energy. Furthermore, it should be mentioned that we have chosen to use rigid

TABLE 2: Equilibrium Position on the Potential Energy Curves (PEC) for the *cis*-DDP–Water Interacting System^a

	without BSSE correction		with BSSE correction	
	$r_{eq}(\text{Pt}\cdots\text{O}_w)/\text{\AA}$	$U_Q/\text{kcal}\cdot\text{mol}^{-1}$	$r_{eq}(\text{Pt}\cdots\text{O}_w)/\text{\AA}$	$U_Q^{CP}/\text{kcal}\cdot\text{mol}^{-1}$
PEC1	3.35	−1.11		
PEC2	3.35	−8.73	3.65	−4.49
PEC3				
PEC4	4.10	−7.90	4.25	−5.67
PEC5	4.70	−2.71	5.00	−0.93
PEC6	4.70	−5.03	5.00	−3.59
PEC7	4.10	0.04		
PEC8	5.45	−0.50		

^a Data with and without BSSE correction are included.

monomers in the PECs calculations and it is expected that the BSSE effect is larger in this situation. To investigate the error introduced by using rigid monomers, we reoptimized the equilibrium structure from PEC2, and the BSSE dropped to 57% of the interaction energy, compared to 94% when rigid monomers are taken. Nevertheless, the approach used here allows the developed potential to be used in rigid-body MC simulation, so hereafter we discuss only the results from the BSSE-corrected PECs. The PEC1 was found to be slightly repulsive, and for PEC2 the equilibrium distance $r(\text{Pt}\cdots\text{O}_w)$ was 3.65 Å, with the interaction energy equal to −4.49 kcal/mol. These results follow the same trend found for interaction between the neutral complex $[\text{Pt}(\text{NH}_3)_2(\text{OH})_2]$ and water reported by Kozelka and colleagues.⁵² In that study, approach I (our PEC1) was purely repulsive, whereas in approach II (our PEC2) the minimum corresponds to a bound state with a depth of 4 kcal·mol^{−1}. There are some experimental evidences of intramolecular $\text{Pt}(\text{II})\cdots\text{H}-\text{X}$ ($\text{X} \equiv \text{C}, \text{N}, \text{O}$) interactions,⁵³ which have also been considered in the force field parametrization.⁵⁴ The conclusion drawn from these observations is that this kind of interaction should not have a great contribution to the stabilization of the molecular systems because of a sort of balance between attractive and repulsive $\text{Pt}\cdots\text{H}$ forces. In the case of intermolecular interactions (PEC2), the close contact and greater stabilization might be attributed to the use of frozen geometry for the complex. When the complex geometry from the minimum point of PEC2 was fully optimized, the structure has undergone a significant distortion in order to relieve the $\text{HO}-\text{H}\cdots\text{Pt}$ repulsion. The final geometry showed a $r(\text{Pt}\cdots\text{O}_w)$ distance of 3.2 Å with $\angle \text{Pt}\cdots\text{H}-\text{OH} = 119^\circ$, with the water molecule moving toward the NH_3 ligand, participating in two weak hydrogen bonds ($r(\text{O}\cdots\text{H}\text{NH}_2) = 2.18$ Å).

From the other PECs depicted in Figure 2, it can be seen that for the orientations 3, 7, and 8 no minima were found. Arrangement 4 (PEC4) is also very stabilized (−5.67 kcal/mol) although the equilibrium distance was longer than that in structure 2: $r(\text{Pt}\cdots\text{O}_w) = 4.25$ Å. This stabilization is due mainly to the hydrogen bonds with the amine groups. This is also the case for structures 5 (PEC5) and 6 (PEC6) where the $\text{H}_2\text{O}\cdots\text{H}-\text{NH}_2$ and $\text{HO}-\text{H}\cdots\text{Cl}$ hydrogen bonds play an important role in the stabilization energy (−0.93 and −3.59 kcal/mol, respectively, for 5 and 6). The effect of basis set on the PECs was analyzed by carrying out calculations at higher level of theory, MP2/6-31++G(d,p)/LANL2DZ, including a set of seven *f* functions ($\alpha_f = 0.9804$)⁵⁰ added to the Pt center. The stabilization energies were slightly lower, found to be −5.08 (PEC2), −5.78 (PEC4), −0.99 (PEC5), and −3.81 kcal/mol (PEC6) (see Table 2 for comparison). As expected, the BSSE also decreased with the basis-set improvement; however, it still plays a primary role in the interaction energy. Therefore, because no significant

changes were observed, we kept the MP2/6-31G(d,p)/LANL2DZ values as reference data for the parametrization procedure.

Although the systems were considered frozen to the construction of the PECs in Figure 2, we assumed that these PECs are good as reference data for the parametrization of the intermolecular Lennard-Jones potential. The procedure involved the fitting of σ and ϵ parameters for all atoms of cisplatin simultaneously keeping the values for water the same as those from the TIP3P model.⁴⁰ The charges were not fitted; ChelpG values were used for cisplatin atoms, and TIP3P values were used for water (see Table 1). The ChelpG charges were used here following our previous studies on MC simulation of organic molecules.^{25–28} Recently, Burda and co-workers⁵¹ showed that the Pt partial charges from the ChelpG approach are too small compared to those from the natural population analysis (NPA). For the *cis*-DDP molecule, we calculated q_{Pt} equal to 0.64e (NPA) and 0.069e (ChelpG) as pointed out in ref 51. However, as discussed in the next paragraph, the Lennard-Jones plus Coulomb parameters (eq 1) must be used as a unique set; therefore, there is not a basic problem with the use of the ChelpG charges.

The first attempt to fit the Lennard-Jones parameters for cisplatin atoms were done considering all points on the PECs, and no convergence could be reached. Then, the reference data set was reduced taking only the interaction energies lower than 6 kcal/mol, which yielded an f value of 0.54 (see Table 1). The individual error was always lower than 0.9, being more pronounced on PECs 2 ($f = 0.84$) and 6 ($f = 0.82$). In PEC2, the O–H bond vector is orientated toward the Pt center along the z axis (see Figure 1b). As pointed out by Kozelka in ref 52, the dispersion component is the main term in this interaction and the Lennard-Jones part of the potential should play a primary role in the classical interaction energy. The ϵ parameter for the Pt atom dictates the quality of fitting of PECs 2 and 1. For example, a larger value of $\epsilon_{\text{Pt}} = 3.0550 \text{ kcal}\cdot\text{mol}^{-1}$ decreases f for PEC2 from 0.84 to 0.12, whereas the error on PEC1 rises from 0.63 to 2.53. However, if ϵ_{Pt} is set to a smaller value of $0.0550 \text{ kcal}\cdot\text{mol}^{-1}$, then the errors on PECs 2 and 1 are 3.31 and 0.22, respectively. A similar analysis could be done for PEC 6, and in this case the σ parameter for chloride plays a primary role in fitting the procedure. If the actual value of 4.6272 Å (Table 1) is changed to 4.9272 Å, then the error on PEC6 drops to 0.06, but the error on PEC5 increases from 0.70 to 3.58. The best value of σ_{Cl} for PEC5 is 4.5272 Å, given $f = 0.22$. The errors on the other PECs are not affected much by these changes, and the parameters in Table 1 represent average values that minimize the overall f function. The fitted potential is compared with the reference data for cisplatin in Figure 2 where a satisfactory overall agreement for all PECs can be seen.

The Lennard-Jones parameters reported in Table 1 for cisplatin atoms are somewhat distinct from those described in the literature. For the Pt atom, our values are $\epsilon = 1.0550 \text{ kcal/mol}$ and $\sigma = 3.6590 \text{ Å}$, which differ from the UFF⁵⁵ (0.080 kcal/mol and 2.754 Å) and AMBER⁵⁶ (0.4 kcal/mol and 4.88 Å) force field parameters. For the other interaction sites, our values are also distinct as can be found in ref 57 for chloride (0.374 kcal/mol and 3.52 Å) and ref 58 for nitrogen (0.17 kcal/mol and 3.25 Å) and hydrogen (0.00 kcal/mol and 0.00 Å) atoms. Two points must be raised in this regard; first is that in the functional form of the Lennard-Jones potential the parameters appear as a geometric average (eq 1), so the values of the parameters for system A (cisplatin) depend on the set of parameters for system B (water), which were equal to the TIP3P model in the present work. The second point is that the

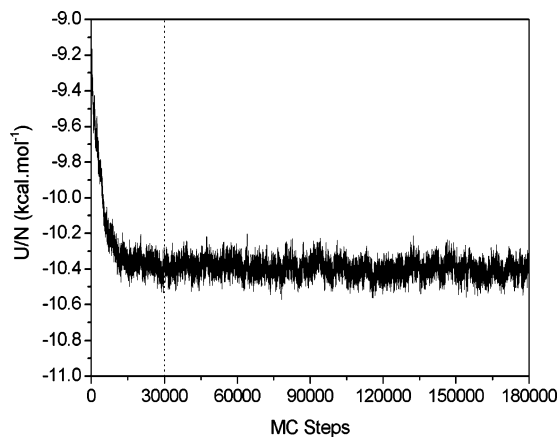


Figure 3. Potential energy per molecule (U/N) calculated for the cisplatin–water system through MC simulation using the classical Lennard-Jones potential from the present work. The dotted vertical line indicates the limit between the thermalization and average phases.

parameters for all atoms must be fitted simultaneously once the interaction energy depends on the whole molecule. When we attempted to adjust the parameters only for platinum atom in cisplatin (keeping the values for Cl, N, and H from refs 57 and 58), no convergence was reached; and if the oxygen from water was also considered in the fitting procedure we found average values for σ_{O} and ϵ_{O} quite different from those for the well-established TIP3P solvent model,⁴⁰ so they cannot be used for liquid and solution simulations without validation. We preferred to keep the solvent unchanged and fit the parameters only for the solute as described previously.

To test the quality of the cisplatin–water intermolecular potential adjusted in the present work, the solvation process of the cisplatin molecule was studied through MC simulation. The simulation protocol (detailed in the Calculation section) was the same as that described by Coutinho and Canuto^{59–65} and also used successfully in our group for oxocarbons and their metal complexes,^{25–28} with the Lennard-Jones parameters for all atoms on cisplatin fitted to reproduce the quantum mechanical PES for the interaction with water (see Table 1). The original TIP3P water model⁴⁰ and the gas-phase MP2/6-31G(d,p)/LANL2DZ optimized geometry for cisplatin were considered frozen throughout the simulation. This latter simplification is supported by the recent DFT Car–Parrinello simulation of cisplatin in water carried out by Carloni and co-workers,²⁹ where it was shown that the vacuum and aqueous solute structures were quite similar.

In Figure 3, the potential energy per molecule (U/N) as a function of the configuration number is shown for the thermalization and average phases. The equilibrium average potential energy per molecule was $-10.39 \pm 0.04 \text{ kcal/mol}$, and the solute–solvent average interaction energy (ΔU^{solv}) was equal to $-28 \pm 3 \text{ kcal/mol}$. These values cannot be compared directly with the data available from the literature.^{20,29–31} Furthermore, the well-behaved energy is a qualitative indication of the quality and stability of our potential. The solution structure was analyzed by calculating the pair correlation functions [$g(r)$] for distinct solvent–solvent and solute–solvent sites. Although we have used the well-known TIP3P model for water,⁴⁰ the structure of solvent on solution was checked to account for the effect of our parametrization. The $g(r)_{\text{O}_w \cdots \text{O}_w}$ and $g(r)_{\text{O}_w \cdots \text{H}_w}$ functions are depicted in Figure 4 and show the first peaks centered at 2.75 and 1.85 Å, respectively, in perfect agreement with the experiment (2.8 and 1.9 Å⁶⁶). The best way to define the solute solvation shells is through the analysis of the $g(r)$

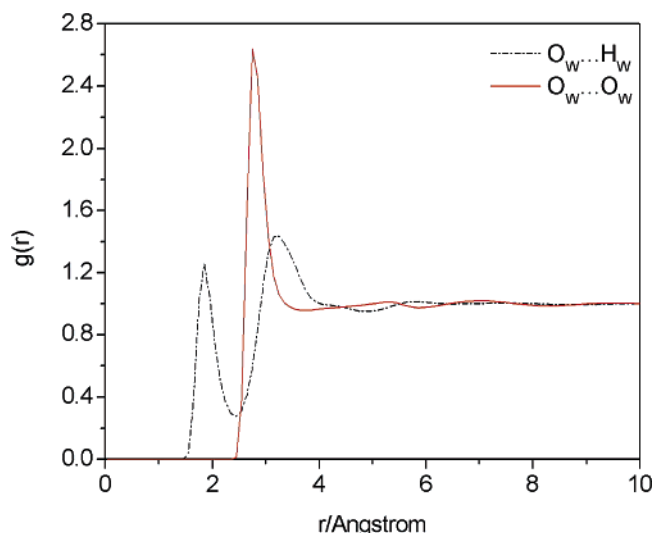


Figure 4. Pair correlation functions for water in the cisplatin solution. The first peaks are centered at 1.85 ($O_w \cdots H_w$) and 2.75 Å ($O_w \cdots O_w$).

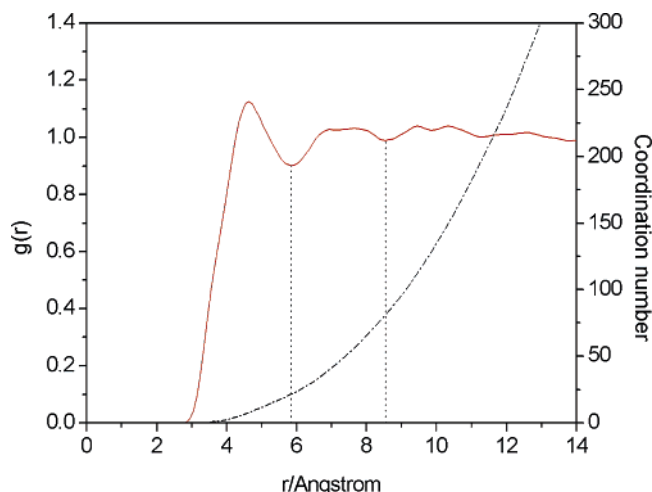


Figure 5. Center of mass pair correlation function for the cisplatin in water with the dotted vertical lines indicating the limits between the solvation shells. The dashed line is relative to the right axis and gives the coordination number as a function of the distance.

for the center of masses (cm) of the solute and solvent. Figure 5 shows this $g(r)$, where two clearly defined hydration shells can be seen, with the second one being more diffuse. Similar results have also been reported for $[PtCl_6]^{2-}$ and $[PtCl_4]^{2-}$ complexes.³¹ For cisplatin, the first solvation shell starts at 2.75 Å and goes up to 5.85 Å with a peak at 4.65 Å, and the second

one is centered at 7.3 Å and extends up to 8.55 Å. The coordination numbers calculated for the first and second solvation shells were 21.6 and 81.0 water molecules, respectively. In Figure 6, some snapshots from the MC simulation of the first hydration shell of cisplatin are depicted, clearly showing that the water molecules are more frequently close to the amine groups. This result will be discussed in detail later considering a larger set of MC configurations. In the DFT Car–Parrinello MD simulation described in ref 29, a box of 10.5 Å with 35 water molecules was treated, which, according to our present results, almost corresponds to the first-solvation shell. For the $[PtCl_4]^{2-}$ complex,³¹ the first solvation shell was defined from the $g(r)$ $Pt \cdots O_w$ and extends from 3.5 to 5.5 Å with the average interatomic distance found to be 3.58 Å. In that study, the number of water molecules that were considered to be the first hydration shell was obtained from the metal \cdots oxygen isoprobability surfaces, being equal to eight solvent molecules on average. In the work of Robertazzi and Platts,²⁰ the estimate of the first solvation shell of cisplatin was 10 water molecules, which is also quite smaller than our prediction (~ 22 solvent molecules). These differences are due mainly to the way the solvation shell is defined. In refs 20 and 31, only the nearest-neighbor water molecules were considered, which corresponds to the number of solute–solvent hydrogen bonds and not to the actual first solvation shell. This is discussed in the last part of the current section.

Figure 7a shows the $g(r)$ $Pt \cdots O_w$ and $Pt \cdots H_w$ pair correlation functions. The overall profile of the $g(r)$ $Pt \cdots O_w$ is very close to the $g(r)$ $cm \cdots cm$, with two peaks centered at 4.45 and 7.3 Å (for the $g(r)$ $cm \cdots cm$ the following values were found: 4.65 and 7.3 Å respectively, see Figure 5). For the $g(r)$ $Pt \cdots H_w$ function two peaks were calculated at 4.95 and 7.45 Å. These results are consistent with the water approaching to the Pt center through the oxygen atom with the closest solvent molecule located at 3.65 Å from the Pt atom and also make clear that the $Pt \cdots H$ interactions (PEC2, Figure 2) do not represent the average behavior of aqueous solution of cisplatin. From the DFT MD simulation,²⁹ the water keeps a minimum distance from Pt always greater than 3.8 Å and for $[PtCl_4]^{2-}$ the average interatomic $Pt \cdots O_w$ distance was 3.58 Å.³¹ It is worth mentioning that the *meso-shell* found for the Pt(II) aquaion, $[Pt(H_2O)_4]^{2+}$, and characterized by a peak around 2.9 Å on the $Pt \cdots O_w$ radial function³⁴ was not observed for cisplatin molecule. According to Martínez and co-workers,³⁴ this hydration pattern accounts for two water molecules located on the axial region of the complex, whose dynamic behavior may be important to establish the ligand exchange mechanism for such kinds of compounds. Therefore, our results support the proposal

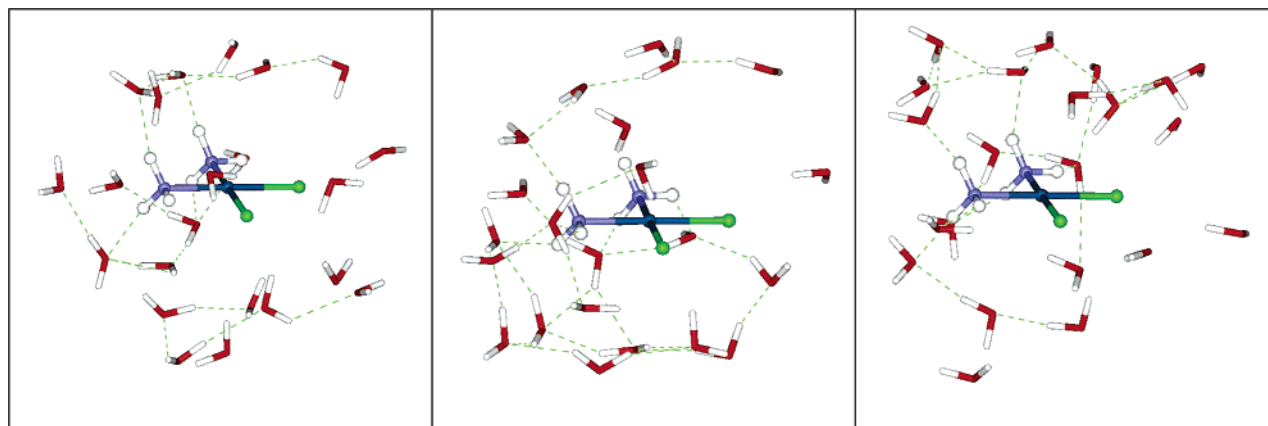


Figure 6. Snapshots selected from the MC simulation for the first solvation shell (22 water molecules).

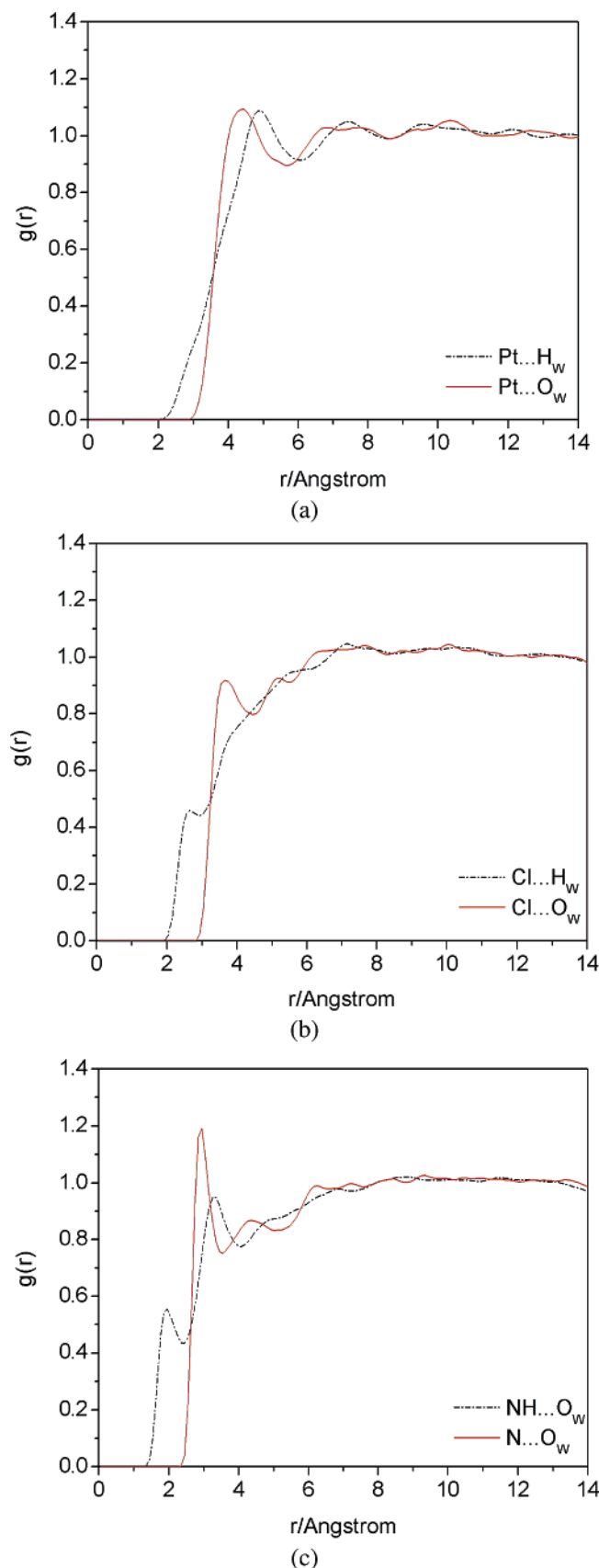


Figure 7. Pair correlation functions calculated from MC simulations.

from ref 34 that the *meso-shell* is a specific hydration pattern of square-planar aquaions and should not be observed for square-planar neutral complexes as cisplatin.

The main hydrogen bonds occur with the Cl and NH₃ ligands in the cisplatin molecule. It can be first qualitatively analyzed

TABLE 3: Average Interatomic Distance (\bar{r}) and Coordination Number Calculated from the Pair Correlation Functions, $g(r)$, for the Cisplatin/Water System

$g(r)$	$\bar{r}/\text{\AA}$		coordination number ^a
	1st peak	2nd peak	
cm...cm	4.65	7.3	21.6 [81.0] ^b
Pt...O _w	4.45	7.3	18.9 [84.1] ^b
Pt...H _w	4.95	7.45	24.5
Cl...O _w	3.65		6.8
Cl...H _w	2.65		0.92
NH...O _w	1.95	3.35	0.8
N...O _w	2.95	4.35	3.6

^a The coordination number was calculated from the integral over the limits of the first peak. ^b The values in brackets correspond to the coordination number also considering the second peak. For the $g(r)$ cm...cm, this is the number of water molecules up to the second solvation shell.

from the $g(r)$ Cl...O_w and Cl...H_w functions shown in Figure 7b and from the $g(r)$ NH...O_w and $g(r)$ N...O_w functions depicted in Figure 7c. The profile of the $g(r)$ calculated for the Cl atoms (Figure 7b) shows that this site is somehow involved in hydrogen bonds with the solvent molecules, with rather well-defined peaks centered at 2.65 (Cl...H_w) and 3.65 Å (Cl...O_w). The integration up to 2.95 Å in $g(r)$ Cl...H_w gives 0.92 water molecules on average hydrogen bonded to each Cl site (Figure 7b). This finding is partially supported by the experimental analysis reported in ref 67 where it was shown that 87% of metal-bound chloride forms short (strong) hydrogen bonds, with $r(\text{Cl}\cdots\text{H})$ being shorter than 2.52 Å. In this same work, the intermediate and long hydrogen bonds were also quoted with $r(\text{Cl}\cdots\text{H})$ ranging from 2.52 to 2.95 Å (intermediate) and greater than 2.95 Å (long). Our results can also be compared to the available theoretical data reported in refs 29–32. In the DFT Car–Parrinello MD simulation,²⁹ the first peak in the $g(r)$ Cl...H_w was found from ~2–2.5 Å with intensity close to 0.8 and the integration gave a coordination number equal to 1.1 water molecule per chloride ligand. This quantum mechanical result is in agreement with our classical MC simulation (see Figure 7b). In the classical MD simulation carried out for [PtCl₄]²⁻ in ref 31, the pair correlation function for Cl...O_w showed two peaks centered at ~3 and ~6 Å, which are close to the values found for the cisplatin molecule in the present work. The results from the QM/MM hybrid method³² also showed that every chloride ligand in general forms ~1 hydrogen bond. The NH₃ ligands are the main groups in the cisplatin molecule involved in hydrogen bonds with the solvent. The $g(r)$ functions depicted in Figure 7c show an overall profile characteristic of hydrogen bonds (compare Figures 4 and 7c) with peaks at 1.95 (NH...O_w) and 2.95 Å (N...O_w), which define the average distances of the hydrogen bonds. The integration up to 2.45 Å in $g(r)$ NH...O_w gives 0.8 water molecules on average for every H atom on the NH₃ moiety, which is in agreement with the quantum mechanical results:²⁹ 2.5 water molecules per NH₃ group, and with QM/MM outcome³² ~3. Then, by summarizing the results from the pair correlation functions we found ~1 hydrogen bond for each chloride with an average Cl...H_w distance equal to 2.65 Å and ~1 hydrogen bond for each hydrogen atom from the NH₃ group with an average H...O_w distance calculated to be 1.95 Å. The data are grouped in Table 3.

To calculate the hydrogen-bond energy and other properties of the solute molecule in the presence of the solvent, we selected some representative configurations of the solution. From the simulation procedure described in the Calculation section, a total of 750 configurations were stored for subsequent analysis. This is a huge number of supermolecular clusters to be further

TABLE 4: Average Hydrogen-Bond Parameters Calculated from the Uncorrelated MC Configurations

donor/acceptor (X) ^a	$r(\text{X}\cdots\text{O})$ (Å) ^b	$\angle(\text{X}\cdots\text{O}-\text{H})$ (deg) ^b	energy (kcal·mol ⁻¹) ^b	distribution ^c
Pt	3.6 ± 0.1	20 ± 7	-2.4 ± 1.7	6%
Cl	3.5 ± 0.2	17 ± 7	-2.8 ± 1.4	41%
N	3.0 ± 0.3	17 ± 7	-3.4 ± 1.8	53%

^a The Pt and Cl atoms were taken as acceptors and the N from NH₃ was taken as a hydrogen-bond donor. ^b The criteria used to identify a hydrogen bond were the following: $r(\text{X}\cdots\text{O}) \leq 4.0$ Å, $\angle(\text{X}\cdots\text{O}-\text{H}) \leq 30^\circ$, and energy ≤ 0.0 kcal/mol. ^c The total of hydrogen bonds was 1515 in 250 uncorrelated configurations.

analyzed and must be reduced using some statistical criteria. In the present study, the uncorrelated configurations were selected according to the elegant methodology proposed by Coutinho and Canuto^{59–65} in which the correlation step (τ) is calculated from the energy correlation function [$C(t)$] and only the statistically relevant configuration separated by τ are analyzed. This procedure is particularly important to reduce the number of configurations to be submitted to subsequent quantum mechanical calculations aiming to study the solvent effect on spectra and physical-chemical properties of molecules in solution.^{59–65} From the simulation of cisplatin in water, we have found $\tau = 283$ MC steps and we set the correlation interval time as 600 MC steps. Then, 250 MC uncorrelated configurations were selected for further analysis.

The solute–solvent hydrogen bonds were analyzed over 250 uncorrelated configurations and the criteria to classify the hydrogen bonds were $r(\text{X}\cdots\text{O}) \leq 4.0$ Å, $\angle(\text{X}\cdots\text{O}-\text{H}) \leq 30^\circ$, and $E \leq 0$ kcal/mol.^{59–65} The Pt and Cl atoms were labeled as proton acceptors, and the N–H moiety (from NH₃) was labeled as a proton donor. A total of 1515 hydrogen bonds were grouped in this way, with 88 (6%) with Pt, 620 (41%) with Cl, and the most of them, 807 (53%), with the H atoms from the NH₃ ligand. The average number of hydrogen bonds per configuration was 6.1 being 0.35 with Pt, 1.24 with each Cl, and 0.54 with each H, which is in good agreement with our previous analysis of the $g(r)$ functions that showed 0.9 and 0.8 water molecules hydrogen bonded to each Cl and H atoms, respectively. The value of 6.1 hydrogen bonds per configuration also agrees with the “first solvation shell” proposed in references 20 and 31. It is important to remember that the $g(r)$ represents an average result over 30 000 configurations and the analysis discussed here is over a smaller set of 250 representative configurations with a hydrogen bond identified according to the criteria specified above. An interesting outcome is that the hydrogen atoms from the in-plane N–H groups, which are aligned toward Cl, are involved in only 0.2 hydrogen bonds on average with the solvent, which is around a third of the value found for the other hydrogen atoms, ~ 0.7 . A quantitative description of hydrogen bonds was done by calculating the distance and energy of hydrogen bonds over the set of 250 uncorrelated configurations (see Table 4). For the Pt atom the Pt \cdots O_w distance was 3.6 ± 0.1 Å and the classical interaction energy was equal to -2.4 ± 1.7 kcal/mol. For the Cl and NH₃ moiety, the hydrogen bonds are slightly shorter and stronger, with Cl \cdots O_w and N \cdots O_w average distances equal to 3.5 ± 0.2 and 3.0 ± 0.3 Å and the hydrogen-bonding interaction energies were calculated to be -2.8 ± 1.4 (Cl \cdots HOH) and -3.4 ± 1.8 kcal/mol (N–H \cdots OH₂). In ref 31, Robertazzi and Platts used the atoms in molecules (AIM) theory to decompose the overall interaction energy in individual contributions. The hydrogen-bond energies were then calculated for each group in cisplatin–water clusters of distinct sizes. In the 1:1 cluster, the N–H \cdots O_w and O–H_w·

·Cl interaction energies were 9.13 and 7.47 kcal/mol, respectively, and when a larger cluster was taken (10:1, water/cisplatin) the average hydrogen-bond energies dropped to 8.09 (N–H \cdots O_w) and 6.05 kcal/mol (O–H_w·Cl). These values are consistent with ours once shorter hydrogen bonds and consequently higher interaction energies for small clusters in the gas phase are expected.

Conclusions

In the present study, the intermolecular Lennard-Jones (12–6) potentials were fitted to reproduce the interaction energy between cisplatin and water molecules. The parametrization protocol considered all atoms of cisplatin simultaneously, and potential energy curves for the water–cisplatin interaction calculated at the MP2/6-31G(d,p)/LANL2DZ quantum mechanical level of theory (a total of 320 points were calculated) were used as reference data. The ϵ and σ atomic parameters were adjusted simultaneously for all atoms of cisplatin, keeping the values for water the same as those reported for the TIP3P model. The final values were the following ($\epsilon/\text{kcal}\cdot\text{mol}^{-1}$ and $\sigma/\text{\AA}$): 1.0550, 3.6590 (Pt); 0.0381, 4.6272 (Cl); 0.0455, 3.3783 (N); and 0.0185, 0.0936 (H).

The obtained Lennard-Jones potential was then used to study the aqueous solution of cisplatin through Monte Carlo simulation. The simulation (150 000 Monte Carlo steps) was carried out with 1000 water molecules. From the analyses of the pair correlation functions [$g(r)$], it was observed interesting features of the solution structure. Two solvation shells were identified from the $g(r)$ cm \cdots cm, centered at 4.65 and 7.3 Å with a total of 22 and 81 water molecules, respectively. The hydrogen-bond analysis showed that only 6% of hydrogen bonds involve the Pt atom. The NH₃ ligands were the main groups involved in hydrogen bond with water (53%) followed by the Cl atoms (41%). These results are in accordance with the expected behavior for such kinds of molecules and also with the DFT Car–Parrinello simulation of cisplatin in water solution.

Finally, it is important to mention that this is the first time that Lennard-Jones (12–6) parameters are reported for all atoms of cisplatin molecule, allowing the classical simulation of aqueous solution of this group of molecules. Our results provide a way of studying the structures and properties of cisplatin-like molecules and also their biological relevant chemical species and processes in water solution with the explicit description of the solvent, especially for larger derivatives where quantum mechanical simulation is prohibitive.

Acknowledgment. Financial support from the Brazilian Agencies CAPES, CNPq, FAPEMIG, and FINEP are gratefully acknowledged. We express our gratitude to Prof. Sylvio Canuto and Dr. Kaline Coutinho for providing their Monte Carlo simulation program DICE and also for helpful discussions.

References and Notes

- (1) Rosenberg, B.; VanCamp, L.; Krigas, T. *Nature* **1965**, 205, 698.
- (2) Rosenberg, B.; VanCamp, L.; Trosko, J. E.; Mansour, V. H. *Nature* **1969**, 222, 385.
- (3) Hambley, T. W. *Coord. Chem. Rev.* **1997**, 166, 181.
- (4) Wong, E.; Giandomenico, C. M. *Chem. Rev.* **1999**, 99, 2451.
- (5) Jamieson, E. R.; Lippard, S. J. *Chem. Rev.* **1999**, 99, 2467.
- (6) Hambley, T. W.; Jones, A. R. *Coord. Chem. Rev.* **2001**, 212, 35.
- (7) Raber, J.; Zhu, C.; Eriksson, L. A. *J. Phys. Chem. B* **2005**, 109, 11006.
- (8) Bednarski, P. J. *J. Inorg. Biochem.* **1995**, 80, 1.
- (9) Soldatovic, T.; Bugarcic, Z. D. *J. Inorg. Biochem.* **2005**, 99, 1472.
- (10) Chval, Z.; Sip, M. *J. Mol. Struct.: THEOCHEM* **2000**, 532, 59.
- (11) Desoize, B.; Madoulet, C. *Crit. Rev. Onc. Hemat.* **2002**, 42, 317.
- (12) Coley, R. F.; Martin, D. S. *Inorg. Chim. Acta* **1972**, 7, 573.

- (13) Miller, S. E.; Gerard, K. J.; House, D. A. *Inorg. Chim. Acta* **1991**, 190, 135.
- (14) Hindmarsh, K.; House, D. A.; Tumbull, M. M. *Inorg. Chim. Acta* **1997**, 257, 11.
- (15) Arpalahti, J.; Mikola, M.; Mauristo, S. *Inorg. Chem.* **1993**, 32, 3327.
- (16) Mikola, M.; Arpalahti, J. *Inorg. Chem.* **1994**, 33, 4439.
- (17) Jestin, J.-L.; Lambert, B.; Chottard, J.-C. *J. Biol. Inorg. Chem.* **1998**, 3, 515.
- (18) Costa, L. A. S.; Rocha, W. R.; De Almeida, W. B.; Dos Santos, H. F. *J. Chem. Phys.* **2003**, 118, 10584.
- (19) Costa, L. A. S.; Rocha, W. R.; De Almeida, W. B.; Dos Santos, H. F. *Chem. Phys. Lett.* **2004**, 387, 182.
- (20) Robertazzi, A.; Platts, J. A. *J. Comput. Chem.* **2004**, 25, 1060.
- (21) Costa, L. A. S.; Rocha, W. R.; De Almeida, W. B.; Dos Santos, H. F. *J. Inorg. Biochem.* **2005**, 99, 575.
- (22) Burda, J.; Zeizinger, M.; Leszczynski, J. *J. Comput. Chem.* **2005**, 26, 914.
- (23) Benigni, R. *Chem. Rev.* **2005**, 105, 1767.
- (24) Rotzinger, F. P. *Chem. Rev.* **2005**, 105, 2003.
- (25) Junqueira, G. M. A.; Rocha, W. R.; De Almeida, W. B.; Dos Santos, H. F. *Phys. Chem. Chem. Phys.* **2001**, 3, 3499.
- (26) Junqueira, G. M. A.; Rocha, W. R.; De Almeida, W. B.; Dos Santos, H. F. *Phys. Chem. Chem. Phys.* **2002**, 4, 2517.
- (27) Junqueira, G. M. A.; Rocha, W. R.; De Almeida, W. B.; Dos Santos, H. F. *Phys. Chem. Chem. Phys.* **2003**, 5, 437.
- (28) Junqueira, G. M. A.; Rocha, W. R.; De Almeida, W. B.; Dos Santos, H. F. *J. Mol. Struct.: THEOCHEM* **2005**, 719, 31.
- (29) Carloni, P.; Sprik, M.; Andreoni, W. *J. Phys. Chem. B* **2000**, 104, 823.
- (30) Lienke, A.; Klant, G.; Robinson, D. J.; Kock, K. R.; Naidoo, K. *J. Inorg. Chem.* **2001**, 40, 2352.
- (31) Naidoo, K. J.; Klatt, G.; Koch, K. R.; Robinson, D. J. *Inorg. Chem.* **2002**, 41, 1845.
- (32) Dobrogorskaia-Méreau, I. A.; Nemukhin, A. V. *J. Comput. Chem.* **2005**, 26, 865.
- (33) Zhu, C.; Raber, J.; Eriksson, L. A. *J. Phys. Chem. B* **2005**, 109, 12195.
- (34) Torrico, F.; Pappalardo, R. R.; Sánchez-Marcos, E.; Martinez, J. M. *Theor. Chem. Acc.* **2006**, 115, 196.
- (35) Ditchfield, R.; Hehre, W. J.; Pople, J. A. *J. Chem. Phys.* **1971**, 54, 724.
- (36) Hehre, W. J.; Ditchfield, R.; Pople, J. A. *J. Chem. Phys.* **1972**, 56, 2257.
- (37) Hay, P. J.; Wadt, W. R. *J. Chem. Phys.* **1985**, 82, 299.
- (38) Norrby, P.-O.; Brandt, P. *Coord. Chem. Rev.* **2001**, 212, 79.
- (39) Allen, M. P.; Tildesley, D. J. *Computer Simulation of Liquids*; Oxford University Press: Oxford, 1987.
- (40) Jorgensen, W. L.; Chandrasekhar, J.; Madura, J. D.; Impey, R. W.; Klein, M. L. *J. Chem. Phys.* **1983**, 79, 926.
- (41) Breneman, C. M.; Wiberg, K. B. *J. Comput. Chem.* **1990**, 11, 361.
- (42) Boys, S. F.; Bernardi, F. *Mol. Phys.* **1970**, 19, 553.
- (43) *Numerical Recipes in Fortran 77: The Art of Scientific Computing*, 2nd ed.; Vol. 1, 2001.
- (44) Frisch, M. J.; Trucks, G. W.; Schlegel, H. B.; Scuseria, G. E.; Robb, M. A.; Cheeseman, J. R.; Montgomery, J. A., Jr.; Vreven, T.; Kudin, K. N.; Burant, J. C.; Millam, J. M.; Iyengar, S. S.; Tomasi, J.; Barone, V.; Mennucci, B.; Cossi, M.; Scalmani, G.; Rega, N.; Petersson, G. A.; Nakatsuji, H.; Hada, M.; Ehara, M.; Toyota, K.; Fukuda, R.; Hasegawa, J.; Ishida, M.; Nakajima, T.; Honda, Y.; Kitao, O.; Nakai, H.; Klene, M.; Li, X.; Knox, J. E.; Hratchian, H. P.; Cross, J. B.; Bakken, V.; Adamo, C.; Jaramillo, J.; Gomperts, R.; Stratmann, R. E.; Yazyev, O.; Austin, A. J.; Cammi, R.; Pomelli, C.; Ochterski, J. W.; Ayala, P. Y.; Morokuma, K.; Voth, G. A.; Salvador, P.; Dannenberg, J. J.; Zakrzewski, V. G.; Dapprich, S.; Daniels, A. D.; Strain, M. C.; Farkas, O.; Malick, D. K.; Rabuck, A. D.; Raghavachari, K.; Foresman, J. B.; Ortiz, J. V.; Cui, Q.; Liashenko, A.; Piskorz, P.; Komaromi, I.; Martin, R. L.; Fox, D. J.; Keith, T.; Al-Laham, M. A.; Peng, C. Y.; Nanayakkara, A.; Challacombe, M.; Gill, P. M. W.; Johnson, B.; Chen, W.; Wong, M. W.; Gonzalez, C.; Pople, J. A. *Gaussian 03*, revision B.05; Gaussian, Inc.: Wallingford, CT, 2004.
- (45) Metropolis, N.; Rosenbluth, A. W.; Rosenbluth, M. N.; Teller, A. H.; Teller, E. *J. Chem. Phys.* **1953**, 21, 1087.
- (46) Coutinho, K.; Guedes, R. C.; Costa-Cabral, B. J.; Canuto, S. *Chem. Phys. Lett.* **2003**, 369, 345.
- (47) Coutinho, K.; Canuto, S. *DICE: A Monte Carlo Program for Molecular Liquid Simulation*; Univeristy of São Paulo, Brazil, 1997.
- (48) Milburn, G. H. W.; Truter, M. R. *J. Chem. Soc. A* **1966**, 1609.
- (49) Benedict, W. S.; Gailan, N.; Plyler, E. K. *J. Chem. Phys.* **1956**, 24, 1139.
- (50) Burda, J. V.; Zeizinger, M.; Sponer, J.; Leszczynski, J. *J. Chem. Phys.* **2000**, 113, 2224.
- (51) Zimmermann, T.; Zeizinger, M.; Burda, J. V. *J. Inorg. Biochem.* **2005**, 99, 2184.
- (52) Kozelka, J.; Bergès, J.; Attias, R.; Fraita, J. *Angew. Chem., Int. Ed.* **2000**, 39, 198.
- (53) Casas, J. M.; Falvello, L. R.; Fornies, J.; Martín, A.; Welch, A. J. *Inorg. Chem.* **1996**, 35, 6009.
- (54) Hambley, T. W. *Inorg. Chem.* **1998**, 37, 3767.
- (55) Rappé, A. K.; Casewit, C. J.; Colwell, K. S.; Goddard, W. A., III; Skiff, W. M. *J. Am. Chem. Soc.* **1992**, 114, 10024.
- (56) Yao, S.; Plastaras, J. P.; Marzilli, L. G. *Inorg. Chem.* **1994**, 33, 6061.
- (57) Rocha, W. R.; Almeida, K. J.; De Almeida, W. B. *Chem. Phys. Lett.* **2000**, 316, 510.
- (58) Jörgensen, W. L. *BOSS version 3.5, Biochemical and Organic Simulation System*; 1995.
- (59) Coutinho, K.; Oliveira, M. J.; Canuto, S. *Int. J. Quantum Chem.* **1998**, 66, 249.
- (60) Coutinho, K.; Canuto, S.; Zerner, M. C. *J. Chem. Phys.* **2000**, 112, 9874.
- (61) Coutinho, K.; Canuto, S. *J. Chem. Phys.* **2000**, 113, 9132.
- (62) Canuto, S.; Coutinho, K. *Adv. Quantum Chem.* **1997**, 28, 89.
- (63) Coutinho, K.; Canuto, S. *J. Mol. Struct.: THEOCHEM* **2003**, 632, 235.
- (64) Rivelino, R.; Coutinho, S.; Canuto, S. *J. Phys. Chem. B* **2002**, 106, 12317.
- (65) Rivelino, R.; Costa-Cabral, B. J.; Coutinho, K.; Canuto, S. *Chem. Phys. Lett.* **2005**, 407, 13.
- (66) Soper, A. K.; Bruni, F.; Ricci, M. A. *J. Chem. Phys.* **1997**, 106, 247.
- (67) Aullón, G.; Bellamy, D.; Guy Orpen, A.; Brammer, L.; Bruton, E. A. *Chem. Commun.* **1998**, 653.